

A Doppler Map and Mass-Ratio Constraint for the Black-Hole X-Ray Nova Ophiuchi 1977 ¹

Emilios T. Harlaftis, Danny Steeghs, Keith Horne

School of Physics and Astronomy, University of St. Andrews, KY16 9SS, Scotland, UK

Electronic mail: (ehh, ds10, kdh1)@st-andrews.ac.uk

and

Alexei V. Filippenko

Department of Astronomy, University of California, Berkeley, CA 94720-3411

Electronic mail: alex@astro.berkeley.edu

ABSTRACT

We have reanalyzed Keck observations of Nova Oph 1977 to extend the work done by Filippenko et al. (1997), who recently determined a mass function $f(M_x) = 4.86 \pm 0.13 M_\odot$ for the compact object. We constrain the rotational broadening, $v \sin i \leq 79 \text{ km s}^{-1}$, at the 90% confidence level, which gives a mass ratio $q \leq 0.053$. The K-type companion star of Nova Oph 1977 contributes 28–37% of the light at red wavelengths. The abnormal Li I $\lambda 6708$ absorption line from the companion star is not detected ($\text{EW} < 0.12 \text{ \AA}$), in contrast to four other X-ray binaries. An $\text{H}\alpha$ Doppler image of the system shows emission from the companion star in addition to the accretion disk.

¹Based on observations obtained at the W. M. Keck Observatory.

1. INTRODUCTION

Significant progress in demonstrating the existence of compact dark stars more massive than neutron stars (i.e., black holes) has been made over the last decade by studying X-ray novae in quiescence. In some cases, these systems consist of late-type (F5–M2) secondary stars orbiting black holes ($\sim 4\text{--}15 M_\odot$) with periods ranging from 5.1 hours to 6.5 days (see, for example, van Paradijs & McClintock 1995). After the initial outburst of the accretion disk around the black hole, the system returns to quiescence, allowing the photospheric lines of the faint companion (secondary) star to be detected. Radial-velocity studies of the companion star (e.g., Casares, Charles, & Naylor 1992) can then provide the mass function of the black hole,

$$f(M_x) = \frac{PK_c^3}{2\pi G} = \frac{M_x \sin^3 i}{(1+q)^2}, \quad (1)$$

where K_c is the semi-amplitude of the radial velocity of the companion star (mass M_c), M_x is the mass of the black hole, and q is the mass ratio M_c/M_x . Moreover, the value of q can be obtained from the rotational broadening of the companion star, $v \sin i$ (e.g., Marsh, Robinson, & Wood 1994), using the relation

$$\frac{v \sin i}{K_c} = 0.462 [(1+q)^2 q]^{1/3}. \quad (2)$$

This formula is derived by assuming that the spin period of the companion star is locked to the binary period and by using Paczyński’s (1971) relation for R_c/a and $q \ll 1$, where a is the semimajor axis of the orbit.

As summarized by Harlaftis & Filippenko (1997), the advent of the 10-m Keck telescopes has enabled measurement of the mass function and mass ratio for black-hole X-ray transients at magnitude $R \approx 21\text{--}21.5$. The objects studied in detail thus far are GRO J0422+32 (Filippenko et al. 1995b; Harlaftis et al. 1997) and GS 2000+25 (Filippenko et al. 1995a; Harlaftis, Horne, & Filippenko 1996, hereafter HHF). Most recently, Filippenko et al. (1997, hereafter FMLBV) derived a mass function $f(M_x) = 4.86 \pm 0.13 M_\odot$ for the compact object in Nova Ophiuchi 1977 by measuring the radial-velocity semi-amplitude of the K-type companion star ($K_c = 447.6 \pm 3.9 \text{ km s}^{-1}$), consistent with an independent estimate by Remillard et al. [1996; $f(M_x) = 4.0 \pm 0.8 M_\odot$].

The reader should refer to FMLBV for an overview of Nova Oph 1977, a description of the Keck observations with the Low Resolution Imaging Spectrometer (LRIS; Oke et al. 1995), and the derivation of the mass function of the compact object. A total of 18

long-slit CCD spectra were obtained on three nights (1996 May 12, and 1996 July 13, 14; see Table 1 for a log of observations). Here, we perform an analysis similar to the one we undertook for GS 2000+25 (HHF), and further refined for GRO J0422+32 (Harlaftis et al. 1997), in order to determine the rotational broadening of the companion star to Nova Oph 1977 (which gives the system’s mass ratio) and to investigate Doppler maps of the H α emission-line distribution.

2. RADIAL VELOCITIES REVISITED

We re-extracted the 18 spectra using the PAMELA software package. The advantages of the package include optimal extraction, efficient clipping of cosmic rays, and production of statistical uncertainties based on photon counts and CCD readout noise (Horne 1986). The detailed reduction procedure is similar to that presented in HHF.

We dereddened the object spectra by $E(B-V) = 0.9$ mag. Although Griffiths et al. (1978) derived $E(B-V) \approx 0.5$ mag during outburst, use of their value still produced significantly red spectra, yet we would expect a blue continuum because the accretion disk is the dominant light source (see § 3). Considering the small size of the observed wavelength range, on the other hand, we cannot reliably improve upon the Griffiths et al. reddening determination. Since our conclusions are independent of the precise value of the adopted reddening, here we do not further consider it.

Table 2 gives nightly averages of the continuum flux density in the range 6600–6800 Å, the H α emission-line flux integrated between -1900 and $+1900$ km s $^{-1}$ of line center, and the H α equivalent width (EW). As already remarked by FMLBV, the spectrum (continuum and H α profile) changed considerably between the May and July epochs. For example, a typical double-peaked H α profile (with a separation of 980 ± 40 km s $^{-1}$) was present in May, but the line profile on July 14 was unusual, had a much smaller EW, and included a narrow emission line at 6578 Å ($\sim +700$ km s $^{-1}$) whose origin is other than the sky. This feature was also observed at another epoch (July 1994) which suggests that it may be related to the unusual shape of the profile (see Fig. 2 in Remillard et al. 1996). Interestingly, [N II] $\lambda 6583$ is $+270$ km s $^{-1}$ away, but the absence of evidence for [N II] $\lambda 6548$ makes this an unlikely identification.

Results of the new radial-velocity analysis are collected in Table 3 and the salient points are as follows. For K3/4, K5, K7, and M0 template stars, we find $438 < K_c < 441$ km s $^{-1}$, and $-75 < \gamma < -31$ km s $^{-1}$. Note that the derived value of K_c is independent of the template star used. The γ velocities span a larger range than expected from the

uncertainties, perhaps indicating that some of the heliocentric radial velocities of the template stars (taken from the SIMBAD database) are erroneous. We choose the average of the values found for the different templates and use the spread to estimate its uncertainty: $\gamma = -54 \pm 15 \text{ km s}^{-1}$. This is consistent with the result of FMLBV (average $\gamma = -41.1 \pm 0.8 \text{ km s}^{-1}$), but the uncertainty is now considerably more realistic.

We adopt the K5 spectral type, which gives a radial-velocity ephemeris (see § 4)

$$V_R = \gamma + K_c \left[\sin \frac{2\pi}{P}(t - T_0) \right], \quad (3)$$

with $K_c = 441 \pm 6 \text{ km s}^{-1}$, $\gamma = -54 \pm 15 \text{ km s}^{-1}$, $P = 0.5228 \pm 0.0044 \text{ d}$, and $T_0 = \text{HJD } 2,450,212.9800 \pm 0.0092$ (inferior conjunction of the companion star). For comparison, FMLBV found $K_c = 447.6 \pm 3.9 \text{ km s}^{-1}$, $P = 0.5229 \pm 0.0044 \text{ d}$, and $T_0 = \text{HJD } 2,450,212.9641 \pm 0.0038$ (after conversion to the phase convention used here). They adopted 0.5229 d as the best of five periods from a global χ^2 analysis, and assigned an uncertainty of 0.0044 d, equal to the separation between adjacent periods. We tried the orbital solution with $P = 0.5272 \text{ d}$ to test for sensitivity of our results, but found no significant difference in the χ^2 or $v \sin i$ compared to those obtained with $P = 0.5228 \text{ d}$.

3. ROTATIONAL BROADENING OF THE COMPANION STAR

The spectral type, rotational broadening $v \sin i$, and fractional contribution f of the companion star to the total flux can be determined by using the χ^2 statistic after subtracting different template spectra from the Doppler-corrected average spectrum (see § 5 in HHF, and references therein). The steps of this analysis were as follows.

The spectra were rebinned onto a common logarithmic wavelength scale using a “ $\sin x/x$ ” interpolation scheme to minimize data smoothing (Stover et al. 1980). This step provided spectra with a uniform pixel size of 30.1 km s^{-1} , and was used to effectively remove Doppler shifts arising from the Earth’s motion, heliocentric radial velocities of the template stars, and orbital motion of the companion star as computed from the appropriate sinusoidal radial velocity curve (see Table 3).

We then fitted low-order spline functions to the continua, and normalized the spectra by dividing by the fitted continua and subtracting 1. In performing the continuum fits, all points above $+3\sigma$ and below -1.8σ were rejected to make the fits pass close to the continuum rather than being biased downward by numerous absorption lines and TiO bands. This “ σ -clipping” procedure worked well on the template star spectra, but did not

reject enough absorption lines when fitting the individual spectra of Nova Oph 1977, which had lower signal-to-noise (S/N) ratios. We therefore averaged the Nova Oph 1977 spectra to increase the S/N ratio by a factor of ~ 4 . The shape of the continuum obtained from a σ -clipped spline for the mean spectrum was then scaled to fit (and subsequently normalize) the individual spectra of Nova Oph 1977.

We then averaged the Doppler-corrected spectra obtained on 14 July, which had the best S/N ratio and covered half an orbital cycle. In this mean spectrum, absorption features from the companion star are relatively sharp because the Doppler shifts due to orbital motion have been shifted to zero velocity. The lines are still broadened, however, by the rotation of the star, by changes in the orbital velocity during the individual exposures, and by the instrumental resolution of the spectrograph. The instrumental profile (full width at half-maximum [FWHM] = 108 km s^{-1}) is of course the same for the template star and Nova Oph 1977 spectra. Our procedure to estimate the companion star’s rotational broadening parameter $v \sin i$ is therefore to (a) “blur” the template star spectra, to simulate rotational broadening and the residual orbital drifts, (b) scale each blurred template spectrum by a factor f , to fit the mean spectrum of Nova Oph 1977, and finally (c) use the χ^2 statistic to locate the parameter values that give the best fit.

The line broadening function we adopted is the convolution of the rotational broadening profile of a limb-darkened spherical star with rectangular profiles that simulate the velocity drifts during the individual exposures. The velocity drift during an exposure of duration Δt is

$$\Delta V \approx \left| \frac{\partial V_R}{\partial t} \right| \Delta t = \frac{2\pi K_c \Delta t}{P} |\cos \phi|. \quad (4)$$

Table 1 lists the exposure durations $\Delta t \approx 25\text{--}30$ min, the binary phases ϕ , and the corresponding velocity drifts ΔV , which range from 5 to 92 km s^{-1} . The template spectra were convolved with rectangular profiles corresponding to the orbital drifts during each exposure, and then averaged using weights identical to those used to obtain the mean spectrum of Nova Oph 1977.

We adopted the rotational broadening profile of a spherical star (Gray 1976) with $v \sin i$ ranging from 0 to 150 km s^{-1} in steps of 10 km s^{-1} , and limb-darkening coefficient $u = 0.5$. Our data have insufficient quality to support independent estimation of u and $v \sin i$. We note that the systematic error resulting from $u = 0.5 \pm 0.5$ is $\pm 7\%$ in $v \sin i$, smaller than the statistical uncertainties. Marsh, Robinson, & Wood (1994) investigated the effect of the Roche-lobe distortion on the rotational broadening. Their results show that the error we incur by adopting a spherical star is also less than the statistical noise in

our $v \sin i$ estimates.

We scaled each blurred template spectrum by a factor $0 < f < 1$ to match the absorption-line strengths in the Doppler-corrected mean spectrum of Nova Oph 1977, and subtracted one from the other to obtain a spectrum of residuals. At this stage the residuals spectrum showed long-scale trends resulting from small differences in the continuum fits, and short-scale residuals around the absorption lines resulting from the slightly inaccurate fits of the orbital velocity amplitude and rotational broadening parameters. We eliminated the long-term component by applying a high-pass Gaussian filter of $\text{FWHM} = 900 \text{ km s}^{-1}$ (30 pixels), and then computed χ^2 from the high-pass filtered residuals.

Next, values of $v \sin i$ and f were chosen to minimize χ^2 , with results as given in Table 4. At the 90% confidence level, all templates place an upper limit on $v \sin i$ below 79 km s^{-1} . At the 68% confidence level, the templates give upper limits with the exception of the K5 template, which gives a best fit at $v \sin i = 50_{-23}^{+17} \text{ km s}^{-1}$. This is illustrated in Figure 1, which displays χ^2 versus $v \sin i$ for the K5 template. The plot shows a non-Gaussian distribution (χ^2 becomes flatter as $v \sin i$ approaches 0, caused by the finite instrumental resolution) with the above-mentioned minima at the 68% and 90% confidence levels (Lampton, Margon, & Bowyer 1976). Table 4 also shows that the companion star contributes $\sim 26\text{--}37\%$ of the light at red wavelengths; the low end of this range is consistent with the high end of that given by FMLBV (10–30%).

The χ^2 fitting techniques can be used to estimate the spectral type of the companion star, but the best-fit χ^2 values are not necessarily a simple function of spectral type because different noise levels affect our template star spectra. We found that the global χ^2 (sum of 18 values of χ^2 , one for each spectrum of Nova Oph 1977) is similar for all the K-type templates and slightly better than for the M0 template. However, in the average spectrum of Nova Oph 1977 there is no trace of the TiO bands typical of M-type stars. Since the K5 V template gives a clear minimum in the plot of χ^2 versus $v \sin i$ (Fig. 1), we adopt a spectral type of K5 for the companion star. This is consistent with the conclusion of FMLBV, who chose K7 but gave a range of K3–M0.

We also analyzed the data using a more refined technique, which we applied previously to GS 2000+25 (HHF) and GRO J0422+32 (Harlaftis et al. 1997). This technique is basically the same as that described above, except that instead of fitting to a single Doppler-corrected average spectrum of Nova Oph 1977, we subtracted our shifted, blurred, and scaled template star spectra from each of the individual spectra of Nova Oph 1977, using the same $v \sin i$ but 18 different scale factors f for the 18 individual spectra. The plot of global χ^2 versus $v \sin i$ is nearly identical to that derived from analysis of the mean spectrum, and serves to confirm our results. For comparison, the $v \sin i$ derived for the

K5 template is also 50_{-26}^{+18} km s⁻¹. The spectrum at phase 0.25 (smearing of only 5 km s⁻¹ during the exposure) gives $v \sin i = 70_{-53}^{+31}$ km s⁻¹. The individual f values are also consistent within 1σ with those in Table 4.

4. THE K5 V SUBTRACTED SPECTRUM

The procedure applied to the Doppler-corrected average spectrum of Nova Oph 1977 using the K5 V template is illustrated in Figure 2. The spectrum of the K5 V template (HD 125354) is shown at the bottom, binned to 124 km s⁻¹ pixels. This template was processed as described in § 3, and a rotational broadening profile corresponding to $v \sin i = 50$ km s⁻¹ was applied (see Table 4). The result, after multiplication by $f = 0.37$ (Table 4), is the second spectrum from the bottom in Figure 2. The spectrum above it is the Doppler-corrected average of the Nova Oph 1977 data in the rest frame of the companion star. Finally, the residual spectrum shown at the top is the result of subtracting the simulated K5 V template from the Doppler-shifted average spectrum.

The K-star absorption lines are evident in the Doppler-corrected average, and they are almost completely removed by subtraction of the template spectrum (e.g., the Na I D and 6495 Å lines). The residual spectrum brings out disk lines and possible anomalous strengths of companion star lines not removed by the template. Emission from He I $\lambda 5876$ and $\lambda 6678$ is absent. There is also no clear evidence for Li I $\lambda 6708$ absorption to a 1σ EW upper limit of 0.12 Å relative to the observed continuum; this is formally consistent with the marginal detection suggested by FMLBV (EW = 0.08 ± 0.04 Å).

5. THE H α DOPPLER MAP

We used the maximum entropy Doppler tomography method (Marsh & Horne 1988; Harlaftis & Marsh 1996) to reconstruct a Doppler map of H α emission from the set of spectra obtained on July 14 (Fig. 3), when half of an orbital cycle was covered. The trailed spectra in the top panel show a weak double-peaked profile with an “S-wave” component moving from red to blue at phase 0.9. The orbital phases were determined from the ephemeris given in § 2. The double peak is a classical signature of an accretion disk. The constructed tomogram is the simplest image that can reproduce (estimated by the χ^2_ν statistic) our observed line profiles at each phase. The iterative process of building up the image is repeated until convergence at the maximum entropy solution is reached at the desired χ^2_ν value. The final Doppler image was then used to build the predicted spectra

by projecting the image at the observed binary phases (see bottom panel in Fig. 3 for computed spectra).

The Doppler image shows the weak ring-like distribution of an accretion disk (which projects to form the double-peaked line profiles) with emission present at velocities ranging between 300 and 1000 km s⁻¹ (center panel of Fig. 3). The narrow line at 6577 Å causes a narrow ring in the image. At phase 0.9, the effect of the strong “S-wave” component in the spectrum is evident on the image. The path of Keplerian velocities along the gas stream (upper path) and the ballistic trajectory (lower path) are plotted along with the Roche lobe of the companion star (for $q = 0.034$, $K_x = 16$ km s⁻¹). The image suggests that there is emission related to the companion star and possibly the gas stream. The H α emission line from the companion star is also seen in Figure 2 (top spectrum). The linear intensity scale is common for all panels.

6. DISCUSSION

The velocity semi-amplitude $K_c = 441 \pm 6$ km s⁻¹ and period $P = 0.5228 \pm 0.0044$ d imply a mass function

$$f(M_x) = (4.65 \pm 0.21) M_\odot = \frac{M_x \sin^3 i}{(1 + q)^2}, \quad (5)$$

consistent with the FMLBV estimate of $4.86 \pm 0.13 M_\odot$. The constraint $v \sin i \leq 79$ km s⁻¹ (and with a likely value of $v \sin i = 50_{-23}^{+17}$ km s⁻¹ for a K5 companion star) gives a mass ratio $q \leq 0.053$ ($q = 0.014_{-0.012}^{+0.019}$ for K5) using equation (2). The mass ratio implies $K_x = qK_c \leq 23$ km s⁻¹ ($K_x = 6_{-5}^{+9}$ km s⁻¹ for K5). Note that FMLBV obtained $K_x = 4.5 \pm 1.8$ km s⁻¹ (and $q = 0.01$) by measuring the centroid of the H α emission line. This makes Nova Oph 1977 one of the most extreme mass-ratio systems, comparable to GS 2000+25 ($q = 0.042 \pm 0.012$; HHF).

Remillard et al. (1996) constrained the system inclination to be $60^\circ < i < 80^\circ$, based on the ellipsoidal variations due to the companion star on the one hand and the absence of eclipses on the other hand. For $q = 0.014$ (the formal mass ratio obtained from $v \sin i = 50$ km s⁻¹), the resulting masses of the compact object and companion star are respectively $5.0 < M_x < 7.4 M_\odot$ and $0.07 < M_c < 0.10 M_\odot$ (with a contribution of 26–37% of the light in our red spectra). For comparison, a normal K5 V star has a mass of $0.39 M_\odot$ (Allen 1976). An upper limit to the companion star mass from our upper limit to the mass ratio ($q \leq 0.053$) gives $4.9 < M_x < 7.9 M_\odot$ and $0.26 < M_c < 0.42 M_\odot$ for $q=0.053$.

Undermassive (i.e., evolved) companion stars are not uncommon in black-hole candidates (e.g., Harlaftis et al. 1997, and references therein). McClintock & Remillard (1990) also infer a very low mass companion ($\sim 0.1 M_{\odot}$) in the neutron-star binary Cen X-4.

We do not detect the Li I $\lambda 6708$ line ($EW < 0.12 \text{ \AA}$; 1σ) which has been observed in four X-ray binaries that have similar system properties (e.g., $EW = 0.27 \pm 0.04 \text{ \AA}$ in GS 2000+25; Filippenko et al. 1995a). The absence of Li I in Nova Oph 1977 suggests that it may not be present in all X-ray transients. A similar result was found for GRO J0422+32 which, however, has an M2 companion star (Filippenko et al. 1995b; Harlaftis et al. 1997). In this case, the outburst mechanism (spallation close to the black hole; Martín et al. 1994) may not be a viable model for the presence of lithium on the companion star, and some other mechanism may be responsible. Recent work on cool stars indicates that the Li I abundance may be linked to stellar activity rather than age (Soderblom et al. 1993). The high rotation rates of the companion stars in X-ray transients and tidal effects caused by the primary star may contribute more to Li enhancement. Clearly, we need confirmation of such a low abundance of Li I in a different K-star/black-hole X-ray binary.

Further progress on Nova Oph 1977 requires higher resolution spectra, particularly at orbital phases 0.25 and 0.75 (where the smearing is minimal) to improve the estimate of the rotational broadening and hence the mass ratio. The inclination may also be further constrained by modeling the ellipsoidal modulations of the companion star at infrared wavelengths.

The W. M. Keck Observatory, made possible by the W. M. Keck Foundation, is operated as a scientific partnership between Caltech and the University of California. We thank the observatory staff, as well as T. Matheson, D. C. Leonard, A. J. Barth, and S. D. Van Dyk, for their assistance. The data analysis was carried out at the STARLINK network (St. Andrews node, UK). Use of software developed mainly by T. Marsh is acknowledged. This research has benefitted from the SIMBAD database, operated at CDS, Strasbourg, France. AVF is grateful for support through NSF grant AST-9417213.

Table 1. Journal of Observations

N	1996 Date	UT(mid)	Δt (s)	HJD ^a	ϕ ^b	V_R ^c	ΔV ^d
1	12 May	10:32:44	1800	215.94463	5.6711	-407 ± 30	53
2	12 May	11:03:24	1800	215.96594	5.7119	-511 ± 15	26
3	12 May	12:06:14	1500	216.00957	5.7954	-500 ± 36	26
4	12 May	12:31:56	1500	216.02742	5.8295	-426 ± 22	44
5	13 July	11:47:21	1500	277.99614	124.3714	211 ± 15	64
6	13 July	12:14:10	1630	278.01476	124.4070	159 ± 21	83
7	14 July	06:30:37	1500	278.77614	125.8639	-425 ± 13	61
8	14 July	06:56:41	1500	278.79424	125.8981	-329 ± 28	73
9	14 July	07:22:22	1500	278.81208	125.9322	-271 ± 15	84
10	14 July	07:52:13	1500	278.83281	125.9719	-165 ± 16	91
11	14 July	08:17:54	1500	278.85064	126.0060	-49 ± 11	92
12	14 July	08:43:44	1500	278.86858	126.0403	73 ± 22	89
13	14 July	09:10:50	1500	278.88740	126.0763	128 ± 21	82
14	14 July	09:36:38	1500	278.90532	126.1106	197 ± 15	70
15	14 July	10:17:32	1500	278.93371	126.1649	276 ± 42	47
16	14 July	10:45:46	1800	278.95332	126.2024	328 ± 30	27
17	14 July	11:18:26	1800	278.97599	126.2458	351 ± 19	5
18	14 July	11:51:45	2100	278.99914	126.2901	378 ± 19	32

^aHJD–2,450,000 at midpoint of exposure.

^bBinary phase ϕ , using $P = 0.5228$ d and $T_0 = 2,450,212.9800$.

^cRadial velocities (km s^{-1}) measured by cross-correlation against the K5 template.

^dOrbital broadening (km s^{-1}) using $K_c = 441 \text{ km s}^{-1}$.

Table 2. Average Properties

1996 Date	Spectra	HJD ^a	F_ν ^b	Flux(H α) ^c	EW(H α) ^d
12 May	4	215.97788	0.0351 ± 0.0002	11.5 ± 0.2	65 ± 1
13 July	2	278.00286	0.0117 ± 0.0002^e	1.00 ± 0.07^e	17 ± 1
14 July	12	278.85411	0.0196 ± 0.0001	1.90 ± 0.05	18 ± 0.5

^aHJD–2,450,000 at midpoint of night.

^bContinuum flux density in the range 6600–6800 Å (mJy).

^cH α emission-line flux (10^{-15} erg s⁻¹ cm⁻²).

^dEquivalent width of H α emission (Å).

^eNot photometric value.

Table 3. Results of Radial Velocity Analysis

Star	Spectral type	γ (km s ⁻¹)	K_c (km s ⁻¹)	χ^2 ($\nu=14$)
HD 109333	K3/4 V	-47 ± 7	438 ± 7	23
BD –05°3763	K5 V	-75 ± 5	441 ± 6	24
HD 125354	K7 V	-62 ± 6	438 ± 7	20
BD +42°2296	M0 V	-31 ± 5	439 ± 7	24

Table 4. Optimal Subtraction of Companion Star

Star	Spectral type	$v \sin i^a$	f^b	$\chi^2(\nu=992)$
HD 109333	K3/4 V	≤ 64	0.26 ± 3	670
BD $-05^\circ 3763$	K5 V	≤ 79	0.37 ± 4	676
HD 125354	K7 V	≤ 60	0.30 ± 3	700
BD $+42^\circ 2296$	M0 V	≤ 73	0.30 ± 3	673

^a90% confidence level.

^bFraction of the light that is contributed by the companion star at 6250 Å.

REFERENCES

- Allen, C. W. 1976, *Astrophysical Quantities*, 3d ed. (London: Athlone)
- Casares, J., Charles, P. A., & Naylor, T. 1992, *Nature*, 355, 614
- Filippenko, A. V., Matheson, T., & Barth, A. J., 1995a, *ApJ*, 455, L139
- Filippenko, A. V., Matheson, T., & Ho, L. C., 1995b, *ApJ*, 455, 614
- Filippenko, A. V., Matheson, T., Leonard, D. C., Barth, A. J., & Van Dyk, S. D., 1997, *PASP*, 109, 461 (FMLBV)
- Gray, D. F. 1976, *The Observations and Analysis of Stellar Photospheres* (New York: Wiley-Interscience), 373
- Griffiths, R. E., et al. 1978, *ApJ*, 221, L63
- Harlaftis, E. T., Collier, S., Horne, K., & Filippenko, A. V. 1997, submitted
- Harlaftis, E. T., & Filippenko, A. V., 1997, in *18th Texas Symposium on Relativistic Astrophysics*, ed. A. Olinto, J. Frieman, & D. Schramm (Singapore: World Scientific), in press
- Harlaftis, E. T., Horne, K., & Filippenko, A. V. 1996, *PASP*, 108, 762 (HHF)
- Harlaftis, E. T., & Marsh, T. R. 1996, *A&A*, 308, 97
- Horne, K. 1986, *PASP*, 98, 609
- Lampton, M., Margon, B., & Bowyer, S. 1976, *ApJ*, 208, 177
- Marsh, T. R., & Horne, K. 1988, *MNRAS*, 235, 269
- Marsh, T. R., Robinson, E. L., & Wood, J. H. 1994, *MNRAS*, 266, 137
- Martín, E. L., Rebolo, R., Casares, J., & Charles, P. A. 1994, *ApJ*, 435, 791
- McClintock, J. E., & Remillard, R. A. 1990, *ApJ*, 350, 386
- Oke, J. B., et al. 1995, *PASP*, 107, 375
- Paczyński, B. 1971, *ARA&A*, 9, 183
- Remillard, R. A., Orosz, J. A., McClintock, J. E., & Bailyn, C. D. 1996, *ApJ*, 459, 226

Stover, R. J., Robinson, E. L., Nather, R. E., & Montemayer, T. J. 1980, ApJ, 240, 597

Soderblom, D., Jones, B. F., Balachandran, S., Stauffer, J., Duncan, D., Fedele, S., & Hudon, J. D., 1993, AJ, 106, 1059

van Paradijs, J., & McClintock, J. E. 1995, in X-Ray Binaries, ed. W. H. G. Lewin, J. van Paradijs, & E. P. J. van den Heuvel (Cambridge: Cambridge Univ. Press), 107

Fig. 1

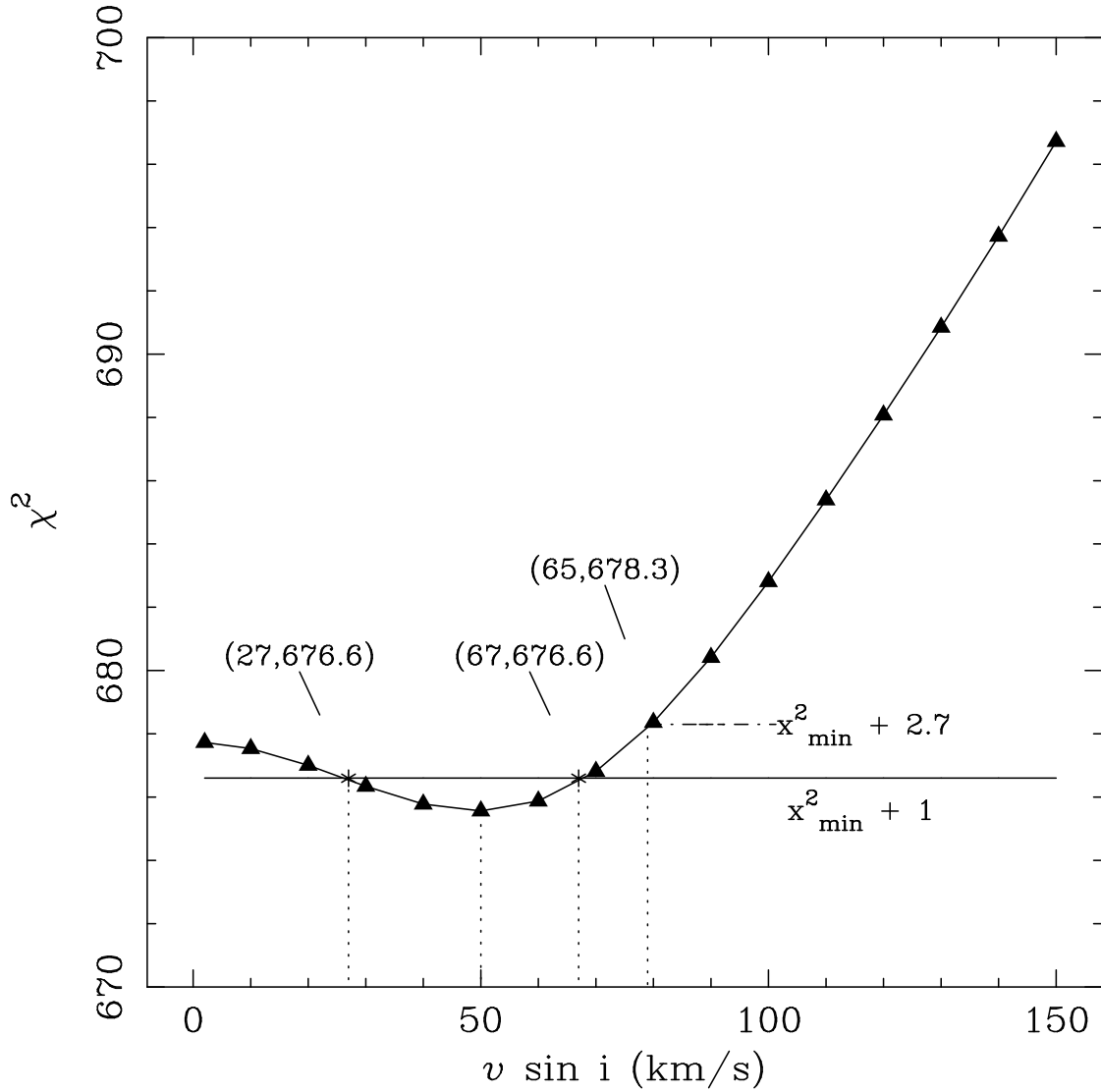


Fig. 1.— The optimal subtraction of the main-sequence template from the Nova Oph 1977 spectra gives a χ^2 distribution for a series of rotational broadenings convolved with the template spectra. The χ^2 distribution for the K5 template (BD $-05^{\circ}3763$) shows a minimum at 50 km s^{-1} . The values for the 68% ($\chi^2_{\min} + 1$) and 90% ($\chi^2_{\min} + 2.7$) confidence levels are marked.

Fig. 2

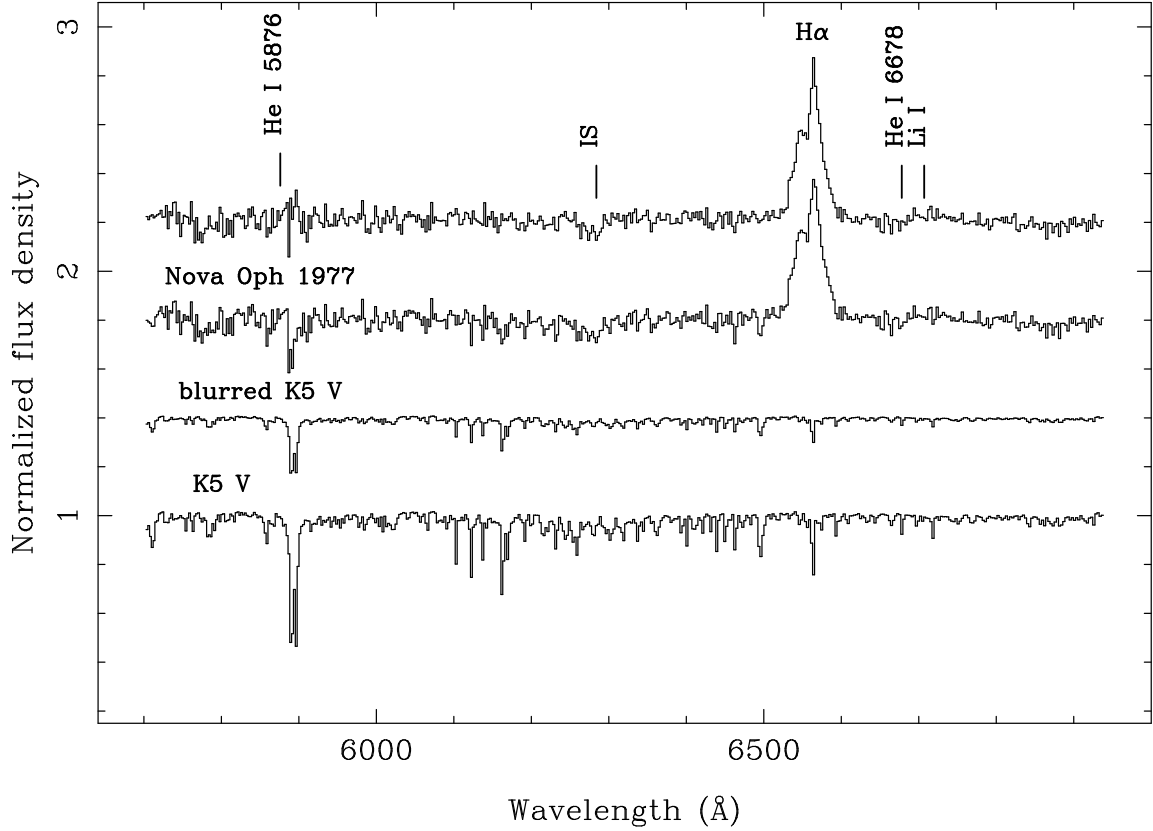


Fig. 2.— Results of the technique followed to extract $v \sin i$ and f for the companion star. From bottom to top are normalized spectra of the K5 V template BD $-05^{\circ}3763$, the K5 V template convolved with a complex profile to simulate effects of orbital smearing and rotational broadening ($v \sin i = 50 \text{ km s}^{-1}$), the Doppler-corrected average spectrum of Nova Oph 1977, and the residual spectrum after subtraction of the template star times $f = 0.37$. All spectra are binned to $124 \text{ km s}^{-1} \text{ pixel}^{-1}$. An offset of 0.4 mJy was added to each successive spectrum for clarity. The residual spectrum is essentially the disk spectrum (featureless continuum, broad $\text{H}\alpha$ emission). An interstellar line is marked (IS), as is the expected position of the undetected $\text{Li I } \lambda 6707.8$ absorption.

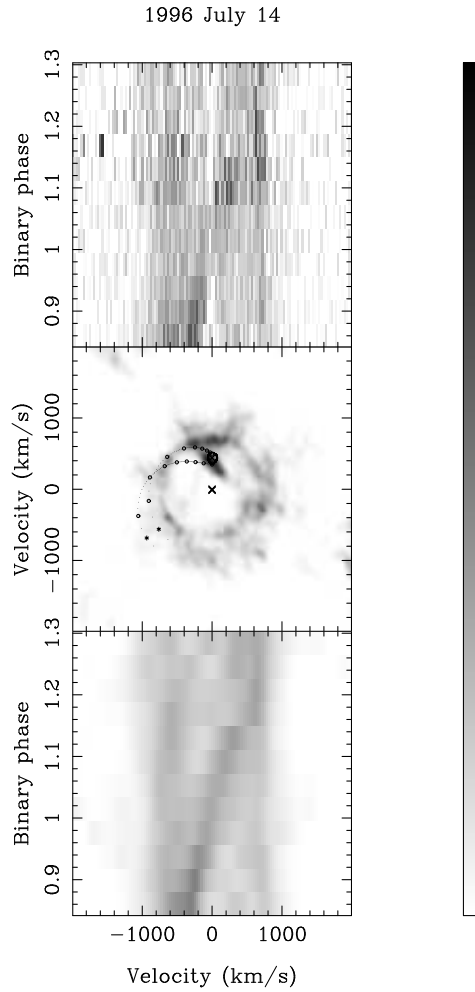


Fig. 3.— Trailed spectra of H α on 1996 July 14 (*top panel*). The ordinate is orbital phase, while the abscissa is velocity relative to the line center. A double-peaked profile is discernible, as is an “S-wave” component crossing from blue to red. The MEM Doppler map (*middle panel*) shows a weak ring typical of accretion disk line distributions and identifies the companion star as the origin of the “S-wave” component. Profiles projected from the image are also displayed (*bottom panel*). See text for details.